

A Degeneracy Framework for Scalable Graph Autoencoders

Guillaume Salha^{1,2}, Romain Hennequin¹, Viet Anh Tran¹ and Michalis Vazirgiannis²

¹Deezer Research & Development, Paris, France

²École Polytechnique, Palaiseau, France

research@deezer.com

Abstract

In this paper, we present a general framework to scale graph autoencoders (AE) and graph variational autoencoders (VAE). This framework leverages graph degeneracy concepts to train models only from a dense subset of nodes instead of using the entire graph. Together with a simple yet effective propagation mechanism, our approach significantly improves scalability and training speed while preserving performance. We evaluate and discuss our method on several variants of existing graph AE and VAE, providing the first application of these models to large graphs with up to millions of nodes and edges. We achieve empirically competitive results w.r.t. several popular scalable node embedding methods, which emphasizes the relevance of pursuing further research towards more scalable graph AE and VAE.

1 Introduction

Graphs have become ubiquitous in the Machine Learning community, thanks to their ability to efficiently represent the relations among items in various disciplines. Social networks, biological molecules, and communication networks are some of the most famous examples of real-world data usually represented as graphs. Extracting meaningful information from such structures is a challenging task that has initiated considerable research efforts, aiming to solve various problems ranging from link prediction to influence maximization and node clustering.

In particular, over the last decade, there has been an increasing interest in extending and applying Deep Learning methods to graph structures. Gori et al. [10] and Scarselli et al. [24] introduced some of the first graph neural network architectures, and were joined by numerous other contributions aiming to generalize CNNs and the convolution operation to graphs, by leveraging spectral graph theory [5], its approximations [8; 15], or spatial-based approaches [13]. Attempts at extending RNNs, GANs, attention mechanisms, or word2vec-like methods to graphs also recently emerged in the literature. For complete references, we refer to Wu et al. [33]’s recent survey on Deep Learning for graphs.

In this paper, we focus on the graph extensions of autoencoders and variational autoencoders. Introduced in the 1980’s [23], autoencoders (AE) are efficient methods to learn low-dimensional “encoded” representations of some input data in an unsupervised way. These models regained significant popularity over the last decade through neural network formulations [1]. Furthermore, variational autoencoders (VAE) [14], described as extensions of AE but actually based on quite different mathematical foundations, also recently emerged as a powerful approach for unsupervised learning from complex distributions. They leverage variational inference techniques, and assume that the input data is the observed part of a larger joint model involving some low-dimensional latent variables. We refer to Tschannen et al. [30] for a review of the recent advances in VAE-based representation learning.

As illustrated throughout this paper, many efforts have been recently devoted to the generalization of such models to graphs. Graph AE and VAE models appear as effective node embedding methods, i.e., methods learning a low dimensional vector space representation of nodes, with promising applications to various tasks including link prediction, node clustering, matrix completion, and graph generation. However, most existing models suffer from scalability issues, and all experiments are currently limited to graphs with at most a few thousand nodes. The question of how to scale graph AE and VAE models to larger graphs remains open. We propose to address it in this paper. More precisely, our contribution is threefold:

- We introduce a general framework to scale graph AE and VAE models, by optimizing the reconstruction loss (for a graph AE) or the variational lower bound objective (for a graph VAE) only from a dense subset of nodes, before propagating the resulting representations in the entire graph. These nodes are selected using graph degeneracy concepts [19]. Such an approach considerably improves scalability while preserving performance.
- We apply this framework to large real-world data and discuss empirical results on ten variants of graph AE and VAE models for two learning tasks. To the best of our knowledge, this is the first application of these models to graphs with up to millions of nodes and edges.
- We show that these scaled models have competitive performances w.r.t. several popular scalable node embedding methods. This emphasizes the relevance of pursuing

ing further research toward scalable graph autoencoders.

This paper is organized as follows. In Section 2, we formally present graph AE and VAE models, as well as their applications and limits. In Section 3, we introduce our “degeneracy” framework to improve the scalability of these models. We describe our experimental analysis and discuss extensions of our approach in Section 4, and we conclude in Section 5.

2 Preliminaries

In this section, we review some key concepts related to graph AE and VAE models. Throughout this paper, we consider an undirected graph $\mathcal{G} = (\mathcal{V}, \mathcal{E})$ with $|\mathcal{V}| = n$ nodes and $|\mathcal{E}| = m$ edges, without self-loops. We denote by A the $n \times n$ adjacency matrix of \mathcal{G} . Nodes can possibly have feature vectors of size $d \in \mathbb{N}^*$, stacked up in an $n \times d$ matrix X . If \mathcal{G} is featureless, then X is the $n \times n$ identity matrix I .

2.1 Graph Autoencoders

Over the last few years, several attempts at extending autoencoders to graph structures with [16] or without [32] node features have been presented. One of the most popular graph AE models is the one from Kipf and Welling [16], often abbreviated as GAE in the literature. In essence, GAE and other graph AE models aim to learn (in an unsupervised way) a low dimensional latent vector space a.k.a. node embedding space (*encoding*), from which reconstructing the graph structure (*decoding*) should be possible. The $n \times f$ matrix Z of all latent vectors a.k.a. embedding vectors z_i (where $f \in \mathbb{N}^*$ is the dimension of the latent space) is usually the output of a Graph Neural Network (GNN) processing A and, potentially, X . To reconstruct A from Z , one could resort to another GNN. However, the GAE model and most of its extensions instead rely on a simpler inner product decoder between latent variables, along with a sigmoid activation function $\sigma(\cdot)$ or, if A is weighted, some more complex thresholding. While being simpler, this decoding involves the multiplication of the two dense matrices Z and Z^T , which has a quadratic complexity $O(fn^2)$ w.r.t. the number of nodes. To sum up, denoting by \hat{A} the reconstruction of A obtained from the decoder:

$$\hat{A} = \sigma(ZZ^T) \quad \text{with} \quad Z = \text{GNN}(A, X).$$

The GNN encoder usually includes weights at each layer. During the training phase, they are optimized by minimizing a reconstruction loss aiming to compare \hat{A} to A , by gradient descent. This loss is often formulated as a Frobenius loss $\|A - \hat{A}\|_F$, where $\|\cdot\|_F$ denotes the Frobenius matrix norm, or alternatively as a weighted cross entropy loss [16].

2.2 Graph Convolutional Networks

In practice, Kipf and Welling [16], and many extensions of their model, assume that this GNN encoder is a Graph Convolutional Network (GCN). Introduced by the same authors in another article [15], GCNs leverage both 1) the features X , and 2) the graph structure summarized by A . In a GCN with L layers, with input layer $H^{(0)} = X$ and output layer $H^{(L)} = Z$, each layer $l \in \{1, \dots, L\}$ computes:

$$H^{(l)} = \text{ReLU}(D^{-1/2}(A + I)D^{-1/2}H^{(l-1)}W^{(l-1)}),$$

i.e., each layer l averages the feature vectors from layer $l - 1$ of the neighbors of each node, and combines them with their own feature vectors along with a ReLU activation function: $\text{ReLU}(x) = \max(x, 0)$. This ReLU is absent from the output layer L . Here, D denotes the diagonal degree matrix of $A + I$, and $D^{-1/2}(A + I)D^{-1/2}$ is therefore the symmetric normalization of $A + I$. $W^{(0)}, \dots, W^{(L-1)}$ are the weight matrices to optimize; they can have different dimensions.

Encoding nodes using a GCN is often motivated by complexity reasons. Indeed, the cost of computing each hidden layer evolves linearly w.r.t. m [15], and the training efficiency of GCNs can also be improved via importance sampling [7]. However, recent works [34] highlighted some fundamental limitations of GCN models, which might motivate researchers to consider more powerful albeit more complex GNN encoders (e.g., [5] computes actual spectral graph convolutions; their model was extended by [8], approximating smooth filters in the spectral domain with Chebyshev polynomials – GCN being a faster first-order approximation of [8]). The scalable degeneracy framework presented in this paper would facilitate the training of such complex models as encoders within a graph AE model.

2.3 Variational Graph Autoencoders

Kipf and Welling [16] also introduced Variational Graph Autoencoders (VGAE). This VAE model for graphs considers a probabilistic model on the graph structure, involving a latent variable z_i of dimension f for each node $i \in \mathcal{V}$. It will be interpreted as the node’s latent vector in the embedding space. More precisely, denoting by Z the $n \times f$ embedding matrix, the inference model (*encoder*) is defined as $q(Z|X, A) = \prod_{i=1}^n q(z_i|X, A)$ where $q(z_i|X, A) = \mathcal{N}(z_i|\mu_i, \text{diag}(\sigma_i^2))$. Parameters of the Gaussian distributions are learned using two two-layer GCNs. Therefore, μ , the matrix of mean vectors μ_i , is defined as $\mu = \text{GCN}_\mu(X, A)$. Also, $\log \sigma = \text{GCN}_\sigma(X, A)$. Both GCNs share the same weights in the first layer. Finally, a generative model (acting as a *decoder*) aims to reconstruct A using the inner product between latent variables: $p(A|Z) = \prod_{i=1}^n \prod_{j=1}^n p(A_{ij}|z_i, z_j)$ where $p(A_{ij} = 1|z_i, z_j) = \sigma(z_i^T z_j)$ and $\sigma(\cdot)$ is the sigmoid function. As in Section 2.1, such a reconstruction has a limiting quadratic complexity w.r.t. n . Kipf and Welling [16] optimize the weights of the two GCNs under consideration by maximizing a tractable variational lower bound (ELBO) of the model’s likelihood:

$$\mathcal{L} = \mathbb{E}_{q(Z|X, A)} \left[\log p(A|Z) \right] - \mathcal{D}_{KL}(q(Z|X, A) \| p(Z)),$$

where $\mathcal{D}_{KL}(\cdot, \cdot)$ is the Kullback-Leibler divergence. They perform gradient descent, using the *reparameterization trick* [14] and choosing a Gaussian prior $p(Z) = \prod_i p(z_i) = \prod_i \mathcal{N}(z_i|0, I)$ [16].

2.4 Applications, Extensions and Limits

GAE and VGAE from Kipf and Welling [16], as well as other graph AE and VAE models, have been successfully applied to various tasks, such as link prediction [16], node clustering [31], and recommendation [3]. Some works also recently tackled multi-task learning problems [29], added adversarial

training schemes enforcing the latent representation to match the prior [21], or proposed RNN-based graph autoencoders to learn graph-level embedding representations [26].

We also note the existence of several applications of graph VAE models to biochemical data and small molecular graphs [18]. Most of them put the emphasis on plausible graph generation using the decoder. Among these models, the ‘‘GraphVAE’’ [25] can reconstruct both 1) the topological graph information, 2) node-level features, and 3) edge-level features. However, it involves a graph matching step with an $O(n^4)$ complexity that prevents the model from scaling, while being acceptable for molecules with tens of nodes.

To the best of our knowledge, all existing experiments on graph AE and VAE models are restricted to small or medium-size graphs, with at most a few thousand nodes and edges. To this date, most models suffer from scalability issues, because they require the training of complex GNN encoders, and/or because they rely on decoders with a quadratic complexity, as Kipf and Welling [16]. This important problem has already been raised, but without applications to large graphs. For instance, Grover et al. [12] proposed ‘‘Graphite’’, a graph AE replacing the decoder with reverse message passing schemes (presented as more scalable), but only reported results on medium-size graphs (up to 20,000 nodes). To summarize this section, graph AE and VAE models showed promising results for small and medium-size datasets, but the question of their extension to large graphs remains widely open.

3 Scaling up Graph AE/VAE with Degeneracy

This section introduces our degeneracy framework to scale graph AE and VAE models to large graphs. In this section, we assume that nodes are featureless, i.e., that models only learn representations from the graph structure (equivalently, $X = I$). Node features will be re-introduced in Section 4.

3.1 Overview of the Framework

To deal with large graphs, the key idea of our framework is to optimize the reconstruction loss (for a graph AE) or the variational lower bound objective (for a graph VAE) only from a wisely selected subset of nodes, instead of using the entire graph \mathcal{G} which would be intractable. We proceed as follows:

1. Firstly, we identify the nodes on which the graph AE/VAE model should be trained, by computing the k -core decomposition of the graph under consideration. The selected subgraph is the so-called k -degenerate version of the original one [19]. We justify this choice in Subsection 3.2 and explain how to choose the value of k .
2. Then, we train the graph AE/VAE model on this k -degenerate subgraph. Hence, we derive latent representation vectors (embedding vectors) for the nodes included in this subgraph, but not for the others.
3. Regarding the nodes of \mathcal{G} that are not in this subgraph, we infer their latent representations using a simple and fast propagation heuristic, presented in Subsection 3.3.

In a nutshell, training the autoencoder (step 2) would still have a high complexity, but now the input graph would be significantly smaller, which would make the training process

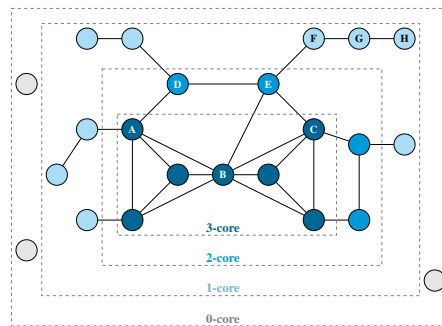


Figure 1: A graph \mathcal{G} of degeneracy 3 and its cores. Some nodes are labeled for the purpose of Section 3.3.

Algorithm 1 k -core Decomposition

Input: Graph $\mathcal{G} = (\mathcal{V}, \mathcal{E})$

Output: Set of k -cores $\mathcal{C} = \{\mathcal{C}_0, \mathcal{C}_1, \dots, \mathcal{C}_{\delta^*(\mathcal{G})}\}$

- 1: Initialize $\mathcal{C} = \{\mathcal{V}\}$ and $k = \min_{v \in \mathcal{V}} d(v)$
 - 2: **for** $i = 1$ **to** n **do**
 - 3: $v =$ node with smallest degree in \mathcal{G}
 - 4: **if** $d(v) > k$ **then**
 - 5: Append \mathcal{V} to \mathcal{C}
 - 6: $k = d(v)$
 - 7: **end if**
 - 8: $\mathcal{V} = \mathcal{V} \setminus \{v\}$ and remove edges linked to v
 - 9: **end for**
-

tractable. Moreover, we will show that steps 1 and 3 have linear running times w.r.t. the number of edges m . Therefore, as we will experimentally verify in Section 4, our strategy significantly improves speed and scalability, and can effectively process large graphs with millions of nodes and edges.

3.2 Graph Degeneracy

In this subsection, we detail the first step of our framework, i.e., the identification of a representative subgraph on which the AE or VAE model should be trained. Our method resorts to the k -core decomposition [2; 19], a powerful tool to analyze the structure of a graph. Formally, the k -core, or k -degenerate version of a graph \mathcal{G} , is the largest subgraph of \mathcal{G} for which every node has a degree larger or equal to k within the subgraph. Therefore, in a k -core, each node is connected to at least k nodes, that are themselves connected to at least k nodes. Moreover, the degeneracy number $\delta^*(\mathcal{G})$ of a graph is the maximum value of k for which the k -core is not empty. Nodes from each core k , denoted $\mathcal{C}_k \subseteq \mathcal{V}$, form a nested chain, i.e., $\mathcal{C}_{\delta^*(\mathcal{G})} \subseteq \mathcal{C}_{\delta^*(\mathcal{G})-1} \subseteq \dots \subseteq \mathcal{C}_0 = \mathcal{V}$. Figure 1 illustrates an example of a k -core decomposition.

In step 2, we therefore train a graph AE or VAE model, either only on the $\delta^*(\mathcal{G})$ -core version of \mathcal{G} , or on a larger k -core subgraph, i.e., for some $k < \delta^*(\mathcal{G})$. Our justification for this strategy is twofold. The first reason is computational: the k -core decomposition can be computed in a linear running time for an undirected graph [2]. More precisely, to construct a k -core, the strategy is to recursively remove all nodes with degrees lower than k and their edges from \mathcal{G} until no node can be removed, as described in Algorithm 1. It involves sorting

nodes by degrees in $O(n)$ time using a variant of bin-sort, and going through all nodes and edges once (see [2] for details). The time complexity is $O(\max(m, n))$ with $\max(m, n) = m$ in most real-world graphs, and with the same space complexity with sparse matrices. Our second reason to rely on the k -core decomposition is that, despite being simple, it has been proven to be a useful tool to extract representative subgraphs over the past years, including for node clustering [9], keyword extraction in graph-of-words [28], and graph similarity via core-based kernels [20]. We refer to Malliaros et al. [19] for an exhaustive overview of the history, theory, and applications of the k -core decomposition.

On the Selection of k . When selecting k , one will usually face a performance/speed trade-off (i.e., choosing small graphs would decrease running times, but also performances), as illustrated in Section 4. Besides, on large graphs ($n > 50,000$), training a graph AE/VAE on the lowest cores would usually be impossible, due to overly large memory requirements. In our experiments, we will adopt a simple strategy when dealing with such large graphs. We will train our graph AE/VAE models on the largest possible subgraphs. In practice, these subgraphs will be significantly smaller than the original ones ($< 5\%$ of nodes). Moreover, when running experiments on medium-size graphs where all cores would be tractable, we will plainly avoid choosing $k < 2$ (since $\mathcal{V} = \mathcal{C}_0 = \mathcal{C}_1$, or $\mathcal{C}_0 \approx \mathcal{C}_1$, in all our graphs). Setting $k = 2$, i.e., removing *leaves* from the graph, will empirically appear as a good option, preserving performances w.r.t. models trained on \mathcal{G} while significantly reducing running times by pruning up to 50% of nodes.

3.3 Propagation of Embedding Vectors

From steps 1 and 2, we compute embedding vectors z_i of dimension f for each node i of the k -core. Step 3 aims to infer such representations for the remaining nodes of \mathcal{G} , in a scalable way. Nodes are assumed to be featureless, so the only information to leverage comes from the graph structure. Our strategy starts by assigning embedding vectors to nodes directly connected to the k -core. We average the values of their embedded neighbors *and* of the nodes being embedded at the same step of the process. For instance, in the graph of Figure 1, to compute z_D and z_E we would solve the system $z_D = \frac{1}{2}(z_A + z_E)$ and $z_E = \frac{1}{3}(z_B + z_C + z_D)$ (or a weighted average, if edges are weighted). Then, we repeat this process on the neighbors of these newly embedded nodes, and so on until no new node is reachable. It is important to consider that nodes D and E are themselves connected. Indeed, node A from the maximal core is also a second-order neighbor of E ; exploiting this proximity when computing z_E empirically improves performance, as it also strongly impacts all the following nodes whose embedding vectors will then be derived from z_E (in Figure 1, nodes F, G and H).

More generally, let \mathcal{V}_1 denote the set of nodes whose embedding vectors are computed, \mathcal{V}_2 the set of nodes connected to \mathcal{V}_1 and without embedding vectors, A_1 the $|\mathcal{V}_1| \times |\mathcal{V}_2|$ adjacency matrix linking \mathcal{V}_1 and \mathcal{V}_2 's nodes, and A_2 the $|\mathcal{V}_2| \times |\mathcal{V}_2|$ adjacency matrix of \mathcal{V}_2 's nodes. We normalize A_1 and A_2 by the total degree in $\mathcal{V}_1 \cup \mathcal{V}_2$, i.e., we divide rows by row sums of the $(A_1^T | A_2)$ matrix row-concatenating

Algorithm 2 Propagation of Embedding Representations

Input: Graph \mathcal{G} , set of embedded nodes \mathcal{V}_1 , $|\mathcal{V}_1| \times f$ embedding matrix Z_1 (already learned), number of iterations t

Output: An embedding vector for each node of \mathcal{G}

- 1: $\mathcal{V}_2 =$ set of not-embedded nodes reachable from \mathcal{V}_1
 - 2: **while** $|\mathcal{V}_2| > 0$ **do**
 - 3: $A_1 = |\mathcal{V}_1| \times |\mathcal{V}_2|$ adj. matrix linking \mathcal{V}_1 and \mathcal{V}_2 nodes
 - 4: $A_2 = |\mathcal{V}_2| \times |\mathcal{V}_2|$ adj. matrix of \mathcal{V}_2 nodes
 - 5: $\tilde{A}_1, \tilde{A}_2 =$ normalized A_1, A_2 by row sum of $(A_1^T | A_2)$
 - 6: Randomly initialize the $|\mathcal{V}_2| \times f$ matrix Z_2 (rows of Z_2 will be embedding vectors of \mathcal{V}_2 's nodes)
 - 7: **for** $i = 1$ **to** t **do**
 - 8: $Z_2 = \tilde{A}_1 Z_1 + \tilde{A}_2 Z_2$
 - 9: **end for**
 - 10: $\mathcal{V}_1 = \mathcal{V}_2$
 - 11: $\mathcal{V}_2 =$ set of not-embedded nodes reachable from \mathcal{V}_1
 - 12: **end while**
 - 13: Assign random vectors to remaining unreachable nodes
-

A_1^T and A_2 . We denote by \tilde{A}_1 and \tilde{A}_2 these normalized matrices. We already learned the $|\mathcal{V}_1| \times f$ embedding matrix Z_1 for nodes in \mathcal{V}_1 . To implement our strategy, we want to derive a $|\mathcal{V}_2| \times f$ embedding matrix Z_2 for nodes in \mathcal{V}_2 , verifying $Z_2 = \tilde{A}_1 Z_1 + \tilde{A}_2 Z_2$. The solution of this system is $Z^* = (I - \tilde{A}_2)^{-1} \tilde{A}_1 Z_1$, which exists since $(I - \tilde{A}_2)$ is strictly diagonally dominant and therefore invertible from the Levy-Desplanques theorem. Unfortunately, the exact computation of Z^* has a cubic complexity. We approximate it by randomly initializing Z_2 with values in $[-1, 1]$ and iterating $Z_2 = \tilde{A}_1 Z_1 + \tilde{A}_2 Z_2$ until convergence to a fixed point, which is guaranteed to happen exponentially fast as stated below.

Theorem 1. *Let $Z^{(t)}$ denote the $|\mathcal{V}_2| \times f$ matrix obtained by iterating $Z^{(t)} = \tilde{A}_1 Z_1 + \tilde{A}_2 Z^{(t-1)}$ t times starting from $Z^{(0)}$, and let $\|\cdot\|_F$ be the Frobenius norm. Then, exponentially fast,*

$$\|Z^{(t)} - Z^*\|_F \xrightarrow{t \rightarrow +\infty} 0.$$

Proof. We have $Z^{(t)} - Z^* = [\tilde{A}_1 Z_1 + \tilde{A}_2 Z^{(t-1)}] - [\tilde{A}_2 Z^* + (I - \tilde{A}_2)Z^*] = \tilde{A}_1 Z_1 + \tilde{A}_2 Z^{(t-1)} - \tilde{A}_2 Z^* - (I - \tilde{A}_2)(I - \tilde{A}_2)^{-1} \tilde{A}_1 Z_1 = \tilde{A}_2 (Z^{(t-1)} - Z^*)$. So, $Z^{(t)} - Z^* = \tilde{A}_2^t (Z^{(0)} - Z^*)$. Then, from the Cauchy-Schwarz inequality, we have:

$$\|Z^{(t)} - Z^*\|_F = \|\tilde{A}_2^t (Z^{(0)} - Z^*)\|_F \leq \|\tilde{A}_2^t\|_F \|Z^{(0)} - Z^*\|_F.$$

Furthermore, $\tilde{A}_2^t = P D^t P^{-1}$, with $\tilde{A}_2 = P D P^{-1}$ the eigendecomposition of \tilde{A}_2 . For the diagonal matrix D^t we have $\|D^t\|_F = \sqrt{\sum_{i=1}^{|\mathcal{V}_2|} |\lambda_i^t|^2} \leq \sqrt{|\mathcal{V}_2|} (\max_i |\lambda_i|)^t$ with λ_i the i -th eigenvalue of \tilde{A}_2 . Since \tilde{A}_2 has non-negative entries, we derive from the Perron-Frobenius theorem [17] that a) the maximum absolute value among all eigenvalues of \tilde{A}_2 is reached by a nonnegative real eigenvalue, and b) that $\max_i \lambda_i$ is bounded above by the maximum degree in \tilde{A}_2 's graph. By definition, each node in \mathcal{V}_2 has at least one connection to \mathcal{V}_1 ; moreover, rows of \tilde{A}_2 are normalized by row sums of $(A_1^T | A_2)$, so the maximum degree in \tilde{A}_2 's graph is strictly

Model	Size of input k -core	Mean Perf. on Test Set (in %)		Mean Running Times (in sec.)				
		AUC	AP	k -core dec.	Model train	Propagation	Total	Speed gain
VGAE on \mathcal{G}	-	83.02 \pm 0.13	87.55 \pm 0.18	-	710.54	-	710.54	-
on 2-core	9,277 \pm 25	83.97 \pm 0.39	85.80 \pm 0.49	1.35	159.15	0.31	160.81	\times 4.42
on 3-core	5,551 \pm 19	83.92 \pm 0.44	85.49 \pm 0.71	1.35	60.12	0.34	61.81	\times 11.50
on 4-core	3,269 \pm 30	82.40 \pm 0.66	83.39 \pm 0.75	1.35	22.14	0.36	23.85	\times 29.79
on 5-core	1,843 \pm 25	78.31 \pm 1.48	79.21 \pm 1.64	1.35	7.71	0.36	9.42	\times 75.43
...
on 8-core	414 \pm 89	67.27 \pm 1.65	67.65 \pm 2.00	1.35	1.55	0.38	3.28	\times 216.63
on 9-core	149 \pm 93	61.92 \pm 2.88	63.97 \pm 2.86	1.35	1.14	0.38	2.87	\times 247.57
DeepWalk	-	81.04 \pm 0.45	84.04 \pm 0.51	-	342.25	-	342.25	-
LINE	-	81.21 \pm 0.31	84.60 \pm 0.37	-	63.52	-	63.52	-
node2vec	-	81.25 \pm 0.26	85.55 \pm 0.26	-	48.91	-	48.91	-
Spectral	-	83.14 \pm 0.42	86.55 \pm 0.41	-	31.71	-	31.71	-

Table 1: Link prediction on the Pubmed graph ($n = 19,717$, $m = 44,338$), using the VGAE model, its k -core variants, and baselines.

lower than 1. We conclude from a) and b) that $0 \leq |\lambda_i| < 1$ for all $i \in \{1, \dots, |\mathcal{V}_2|\}$, so $0 \leq \max_i |\lambda_i| < 1$. This result implies that $\|D^t\|_F \rightarrow_t 0$ exponentially fast, and so does $\|\tilde{A}_2^t\|_F \leq \|P\|_F \|D^t\|_F \|P^{-1}\|_F$, then $\|Z^{(t)} - Z^*\|_F$. \square

Algorithm 2 summarizes our propagation process. If some nodes are unreachable by such a process because \mathcal{G} is not connected, then we assign them random vectors. Using sparse representations for \tilde{A}_1 and \tilde{A}_2 , the memory requirement is $O(m + nf)$, and the computational complexity of each evaluation of line 8 also increases linearly w.r.t. the number of edges m in the graph. Moreover, in practice, t is small: we set $t = 10$ in our experiments (we illustrate the impact of t in Annex 2). The number of iterations in the while loop of line 2 corresponds to the size of the longest shortest path connecting a node to the k -core, a number bounded above by the diameter of the graph, which increases at a $O(\log(n))$ speed in numerous real-world graphs [6]. In the next section, we will empirically check our claim that steps 1 and 3 run linearly and therefore scale to large graphs with millions of nodes.

4 Empirical Analysis

In this section, we empirically evaluate our framework. While all main results are presented here, we report additional and more complete tables in the supplementary material.

4.1 Experimental Setting

Datasets. We provide experiments on the three medium-size graphs used by Kipf and Welling [16]: Cora ($n = 2,708$ and $m = 5,429$), Citeseer ($n = 3,327$ and $m = 4,732$) and Pubmed ($n = 19,717$ and $m = 44,338$); and on two large graphs from Stanford’s SNAP project: the Google web graph ($n = 875,713$ and $m = 4,322,051$) and the US Patent citation network ($n = 2,745,762$ and $m = 13,965,410$). Details, statistics, and k -core decompositions of these graphs are reported in Annex 1. Nodes from Cora, Citeseer, and Pubmed have bag-of-words feature vectors. All graphs are unweighted and, as in [16], we ignore the edges’ directions.

Tasks. We consider two learning tasks. The first one, as in [16], is a *link prediction* task. We train models on incomplete versions of graphs where some edges were randomly

removed. We create some validation and test sets from the removed edges and the same number of randomly sampled pairs of unconnected nodes. We evaluate the model’s ability to classify edges (i.e., the true $A_{ij} = 1$) from non-edges ($A_{ij} = 0$), using the reconstructed value $\hat{A}_{ij} = \sigma(z_i^T z_j)$. The validation and test sets gather 5% and 10% of edges (respectively 2% and 3%) for medium-size (resp. large-size) graphs. The (incomplete) training adjacency matrix is used when running Algorithm 2. The validation set is only used to tune hyperparameters. We compare model performances using the *Area Under the Receiver Operating Characteristic (ROC) Curve (AUC)* and *Average Precision (AP)* scores. The second task consists in *clustering nodes* from embedding representations z_i . We run k -means in embedding spaces, and compare clusters to some ground-truth communities (see Subsection 4.2) using normalized *Mutual Information (MI)* scores.

Models. We apply our degeneracy framework to ten graph autoencoders: the seminal GAE and VGAE models [16] with two-layer GCNs; two deeper variants of GAE and VGAE with 3-layer GCNs; Graphite and Variational Graphite [12]; Pan et al. [21]’s adversarially regularized models (denoted ARG and ARVGA); and ChebAE/ChebVAE, two variants of GAE/VGAE with ChebNets [8] of order 3 instead of GCNs. We train all models during 200 epochs. Models return 16-dimensional embedding vectors (32 for Patent). We also compare to the DeepWalk [22], LINE [27], and node2vec [11] node embedding methods, that are explicitly presented as scalable methods. We tune hyperparameters from AUC scores obtained on the validation set (see Annex 2). We also consider a spectral decomposition baseline (embedding axes are the first eigenvectors of \mathcal{G} ’s Laplacian matrix) and, for node clustering, the scalable ‘‘Louvain’’ method [4]. We use Python, especially the Tensorflow library, training models on an NVIDIA GTX 1080 GPU and running other operations on a double Intel Xeon Gold 6134 CPU.

4.2 Results

Medium-Size Graphs. For Cora, Citeseer, and Pubmed, we apply our framework to all possible subgraphs from the 2-core to the $\delta^*(\mathcal{G})$ -core. We also train models on entire graphs, which is still tractable. Table 1 reports mean AUC and AP

Model (using framework, k=17)	Perf. on Test Set (in %)		Total run. time
	AUC	AP	
GAE	94.02 ± 0.20	94.31 ± 0.21	23min
VGAE	93.22 ± 0.40	93.20 ± 0.45	22 min
DeepGAE	93.74 ± 0.17	92.94 ± 0.33	24min
DeepVGAE	93.12 ± 0.29	92.71 ± 0.29	24min
Graphite	93.29 ± 0.33	93.11 ± 0.42	23min
Var-Graphite	93.13 ± 0.35	92.90 ± 0.39	22 min
ARGA	93.82 ± 0.17	94.17 ± 0.18	23min
ARVGA	93.00 ± 0.17	93.38 ± 0.19	23min
ChebGAE	95.24 ± 0.26	96.94 ± 0.27	41min
ChebVGAE	95.03 ± 0.25	96.58 ± 0.21	40min
node2vec on \mathcal{G} (best baseline)	94.89 ± 0.63	96.82 ± 0.72	4h06

Table 2: Link prediction on the Google graph ($n = 875K$, $m = 4.3M$) using our framework on the 17-core ($|\mathcal{C}_{17}| = 23, 787 \pm 208$) on all graph AE/VAE variants.

scores and their standard errors over 100 runs (training graphs and masked edges are different at each run) along with mean running times, for the *link prediction* task on Pubmed using a VGAE. Sizes of k -cores vary over runs due to the edge masking process in *link prediction*; this phenomenon does not occur for *node clustering*. Overall, our framework significantly improves running times w.r.t. training the VGAE on \mathcal{G} . Running times decrease when k increases (up to $\times 247.57$ speed gain in Table 1), which was expected since the k -core subgraph becomes smaller. We observe this improvement on all other datasets, on both tasks, and for all graph AE/VAE variants (see Annexes 2 and 3). Also, for the low cores, especially the 2-core, performances are consistently competitive w.r.t. models trained on entire graphs, and sometimes better both for *link prediction* (e.g., +0.95 point in AUC for 2-core in Table 1) and *node clustering*. This highlights the relevance of our propagation process, and the fact that training models on smaller graphs is easier. Choosing higher cores leads to even faster running times at the price of a loss in performance.

Large Graphs. Table 2 summarizes *link prediction* results on Google, for all graph AE/VAE variants trained on the 17-core using our framework. Also, in Table 3, we summarize *node clustering* results on Patent. Ground-truth clusters are six roughly balanced patent categories. We report performances for all graph AE/VAE variants trained on the 15-core. Core numbers were selected according to the tractability criterion of Section 3. We average scores over 10 runs. Overall, we reach similar conclusions w.r.t. medium-size graphs, both in terms of good performance and of scalability. However, comparing our results to models trained on \mathcal{G} , i.e., without using our framework, is impossible on these large graphs due to overly large memory requirements. We, therefore, compare results to those obtained on several other cores (see Annexes 2 and 3 for complete tables), illustrating once again the inherent performance/speed trade-off when choosing k and validating previous insights.

Graph AE/VAE Variants. For both tasks, we note that models leveraging adversarial training techniques (ARGA/ARVGA), Graphite’s decoder, or a ChebNet-based

Model (using framework, k=15)	Performance (in %)	Total run. time
	Normalized MI	
GAE	23.76 ± 2.25	56min
VGAE	24.53 ± 1.51	54min
DeepGAE	24.27 ± 1.10	1h01
DeepVGAE	24.54 ± 1.23	58min
Graphite	24.22 ± 1.45	59min
Var-Graphite	24.25 ± 1.51	58min
ARGA	24.26 ± 1.18	1h01
ARVGA	24.76 ± 1.32	58min
ChebGAE	25.23 ± 1.21	1h41
ChebVGAE	25.30 ± 1.22	1h38
node2vec on \mathcal{G} (best baseline)	24.10 ± 1.64	7h15

Table 3: Node clustering on the Patent graph ($n = 2.7M$, $m = 13.9M$) using our framework on the 15-core ($|\mathcal{C}_{15}| = 35, 432$) on all graph AE/VAE variants.

encoder, tend to perform slightly better than others (e.g., a top 95.24% AUC score for ChebGAE in Table 2). This indicates the relevance of these approaches on our two tasks.

Baselines. Additionally, our framework is competitive w.r.t. (non-AE/VAE) baselines. We are significantly faster on large graphs while achieving comparable or outperforming performances in most experiments, which emphasizes the interest of scaling graph AE/VAE models. Furthermore, we specify that 64 dimensions were needed to reach stable results on baselines, against 16 for autoencoders. This suggests that graph AE/VAE models are superior when encoding information in a (very) low-dimensional embedding space. On the other hand, some baselines, e.g., Louvain and node2vec, cluster nodes from Cora and Pubmed more effectively (+10 points in MI for Louvain on Cora), which questions the global ability of existing graph AE/VAE models to identify clusters.

Extensions and Openings. Based on this last finding, our future research will investigate alternative prior distributions for graph VAE models, aiming to detect clusters/communities in graphs. Moreover, while this paper mainly considered featureless nodes, our method easily extends to attributed graphs, since we can add node features from the k -core subgraph as input to graph AE/VAE models. To support this claim, we report experiments on graphs *with node features* for both tasks in Annexes 2 and 3, significantly improving scores (e.g., from 85.24% to 88.10% AUC for the 2-core GAE on Cora). However, node features are currently ignored by our propagation process: future works might, therefore, aim to study more efficient feature integration techniques. Lastly, we aim to obtain theoretical guarantees on k -core approximations and extend our approach to directed graphs.

5 Conclusion

In this paper, we introduced a framework based on graph degeneracy to easily scale graph (variational) autoencoders. We provided experimental evidence of its ability to process large graphs effectively. Our work confirms the representational power of these models and identifies several directions that, in future research, should lead towards their improvement.

References

- [1] Pierre Baldi. Autoencoders, unsupervised learning, and deep architectures. *ICML workshop on unsupervised and transfer learning*, 2012.
- [2] Vladimir Batagelj and Matjaz Zaversnik. An $o(m)$ algorithm for cores decomposition of networks. *arXiv preprint cs/0310049*, 2003.
- [3] Rianne van den Berg, Thomas N Kipf, and Max Welling. Graph convolutional matrix completion. *KDD Deep Learning day*, 2018.
- [4] Vincent Blondel, Jean-Loup Guillaume, and Etienne Lefebvre. Fast unfolding of communities in large networks. *J. Stat. Mech*, 2008.
- [5] Joan Bruna, Wojciech Zaremba, Arthur Szlam, and Yann Lecun. Spectral networks and locally connected networks on graphs. *ICLR*, 2014.
- [6] Deepayan Chakrabarti and Christos Faloutsos. Graph mining: Laws, generators, and algorithms. *ACM computing surveys*, 38(1):2, 2006.
- [7] Jie Chen, Tengfei Ma, and Cao Xiao. Fastgcn: fast learning with graph convolutional networks via importance sampling. *ICLR*, 2018.
- [8] Michaël Defferrard, Xavier Bresson, and Pierre Vandergheynst. Convolutional neural networks on graphs with fast localized spectral filtering. *NIPS*, 2016.
- [9] Christos Giatsidis, Fragkiskos Malliaros, Dimitrios Thilikos, and Michalis Vazirgiannis. Corecluster: A degeneracy based graph clustering framework. *AAAI*, 2014.
- [10] Marco Gori, Gabriele Monfardini, and Franco Scarselli. A new model for learning in graph domains. *IJCNN*, 2005.
- [11] Aditya Grover and Jure Leskovec. node2vec: Scalable feature learning for networks. *SIGKDD*, 2016.
- [12] Aditya Grover, Aaron Zweig, and Stefano Ermon. Graphite: Iterative generative modeling of graphs. *arXiv preprint arXiv:1803.10459*, 2018.
- [13] Will Hamilton, Zhitao Ying, and Jure Leskovec. Inductive representation learning on large graphs. *NIPS*, 2017.
- [14] Diederik P Kingma and Max Welling. Auto-encoding variational bayes. *ICLR*, 2013.
- [15] Thomas N Kipf and Max Welling. Semi-supervised classification with graph convolutional networks. *ICLR*, 2016.
- [16] Thomas N Kipf and Max Welling. Variational graph auto-encoders. *NIPS Workshop on Bayesian Deep Learning*, 2016.
- [17] László Lovász. Eigenvalues of graphs. *Technical report, Eotvos Lorand University*, 2007.
- [18] Tengfei Ma, Jie Chen, and Cao Xiao. Constrained generation of semantically valid graphs via regularizing variational autoencoders. *NeurIPS*, 2018.
- [19] Fragkiskos Malliaros, Christos Giatsidis, Apostolos Papadopoulos, and Michalis Vazirgiannis. The core decomposition of networks: Theory, algorithms and applications. 2019.
- [20] Giannis Nikolentzos, Polykarpos Meladianos, Stratis Limnios, and Michalis Vazirgiannis. A degeneracy framework for graph similarity. *IJCAI*, 2018.
- [21] Shirui Pan, Ruiqi Hu, Guodong Long, Jing Jiang, Lina Yao, and Chengqi Zhang. Adversarially regularized graph autoencoder. *IJCAI*, 2018.
- [22] Bryan Perozzi, Rami Al-Rfou, and Steven Skiena. Deepwalk: Online learning of social representations. *SIGKDD*, 2014.
- [23] David E Rumelhart, Geoffrey E Hinton, and Ronald J Williams. Learning internal representations by error propagation. *Parallel Distributed Processing, Vol 1*, 1986.
- [24] Franco Scarselli, Marco Gori, Ah Chung Tsoi, Markus Hagenbuchner, and Gabriele Monfardini. The graph neural network model. *Neural Networks*, 20(1):61–80, 2009.
- [25] Martin Simonovsky and Nikos Komodakis. GraphVAE: Towards generation of small graphs using vae. *ICANN*, 2018.
- [26] Aynaz Taheri, Kevin Gimpel, and Tanya Berger-Wolf. Learning graph representations with recurrent neural network autoencoders. *KDD DL Day*, 2018.
- [27] Jian Tang, Meng Qu, Mingzhe Wang, Ming Zhang, Jun Yan, and Qiaozhu Mei. Line: Large-scale information network embedding. *WWW*, 2015.
- [28] Antoine Tixier, Fragkiskos Malliaros, and Michalis Vazirgiannis. A graph degeneracy-based approach to keyword extraction. *EMNLP*, 2016.
- [29] Phi Vu Tran. Learning to make predictions on graphs with autoencoders. *DSAA*, 2018.
- [30] Michael Tschannen, Olivier Bachem, and Mario Lucic. Recent advances in autoencoder-based representation learning. *NeurIPS Bayesian DL workshop*, 2018.
- [31] Chun Wang, Shirui Pan, Guodong Long, Xingquan Zhu, and Jing Jiang. Mgae: Marginalized graph autoencoder for graph clustering. *CIKM*, 2017.
- [32] Daixin Wang, Peng Cui, and Wenwu Zhu. Structural deep network embedding. *SIGKDD*, 2016.
- [33] Zonghan Wu, Shirui Pan, Fengwen Chen, Guodong Long, Chengqi Zhang, and Philip S Yu. A comprehensive survey on graph neural networks. *arXiv preprint arXiv:1901.00596*, 2019.
- [34] Keyulu Xu, Weihua Hu, Jure Leskovec, and Stefanie Jegelka. How powerful are graph neural networks? *ICLR*, 2019.

Supplementary Material

This supplementary material provides additional details and more complete tables related to the experimental part of the *A Degeneracy Framework for Scalable Graph Autoencoders* paper. More precisely:

- Annex 1 describes our five datasets and their respective k -core decompositions.
- Annex 2 reports complete tables and experimental settings for the *link prediction* task.
- Annex 3 reports complete tables and experimental settings for the *node clustering* task.

Annex 1 - Datasets

Medium-size graphs

For comparison purposes, we ran experiments on the three medium-size graphs used in [16], i.e., the Cora ($n = 2,708$ and $m = 5,429$), Citeseer ($n = 3,327$ and $m = 4,732$), and Pubmed ($n = 19,717$ and $m = 44,338$) citation networks. In these graphs, nodes are documents and edges are citation links. As [16], we ignored edges' directions, i.e., we considered undirected versions of these graphs. Documents/nodes have sparse bag-of-words feature vectors, of sizes 3,703, 1,433 and 500, respectively. Each document also has a class label corresponding to its topic : in Cora (resp. Citeseer, Pubmed), nodes are clustered in 6 classes (resp. 7 classes, 3 classes) that we used as ground-truth communities for the *node clustering* task. Classes are roughly balanced. Data were collected from Kipf's repository¹ [16].

Large graphs

We also provided experiments on two publicly available large graphs from Stanford's SNAP website. The first one is the Google web graph² ($n = 875,713$ and $m = 4,322,051$), whose nodes are web pages and directed edges represent hyperlinks between these pages. Data do not include ground-truth communities. The second one is the US Patent citation network³ ($n = 2,745,762$ and $m = 13,965,410$), originally released by the National Bureau of Economic Research (NBER) and representing citations between patents. Nodes have classes corresponding to 6 patent categories; we removed nodes without classes from the Patent original graph. For both graphs, we once again ignored edges' directions.

k -core decompositions

Tables 4 to 8 detail the k -core decomposition of each graph. We used the Python implementation provided in the networkx library. For Citeseer, the 1-core is smaller than the 0-core because this graph includes isolated nodes. Figures 2 to 6 illustrate the evolution of the number of nodes in the k -core induced by increasing k . We note that, for Google (resp. for Patent), it was intractable to train autoencoders on the 0 to 15-cores (resp. on 0 to 13-cores) due to memory errors. Therefore, in our experiments, we trained models on the 16 to 20-cores (resp. 14 to 18-cores).

¹<https://github.com/tkipf/gae>

²<http://snap.stanford.edu/data/web-Google.html>

³<http://snap.stanford.edu/data/cit-Patents.html>

k	Number of nodes in k -core	Number of edges in k -core
0	2,708	5,278
1	2,708	5,278
2	2,136	4,768
3	1,257	3,198
4 ($\delta^*(\mathcal{G})$)	174	482

Table 4: k -core decomposition of the Cora graph.

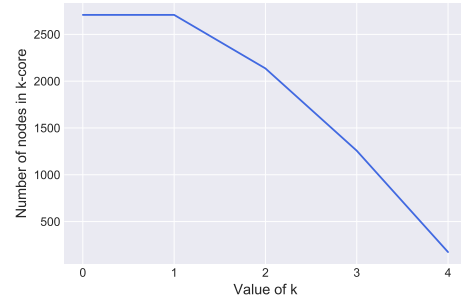


Figure 2: k -core decomposition of the Cora graph.

k	Number of nodes in k -core	Number of edges in k -core
0	3,327	4,552
1	3,279	4,552
2	1,601	3,213
3	564	1,587
4	203	765
5	70	319
6	28	132
7 ($\delta^*(\mathcal{G})$)	18	86

Table 5: k -core decomposition of the Citeseer graph.

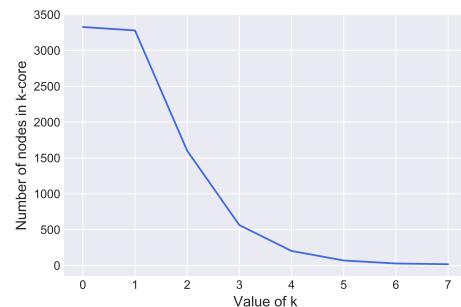


Figure 3: k -core decomposition of the Citeseer graph.

k	Number of nodes in k -core	Number of edges in k -core
0	19,717	44,324
1	19,717	44,324
2	10,404	35,011
3	6,468	27,439
4	4,201	21,040
5	2,630	15,309
6	1,569	10,486
7	937	7,021
8	690	5,429
9	460	3,686
10 ($\delta^*(\mathcal{G})$)	137	1,104

Table 6: k -core decomposition of the Pubmed graph.

k	Number of nodes in k -core	Number of edges in k -core
0	875,713	4,322,051
1	875,713	4,322,051
2	711,870	4,160,100
3	581,712	3,915,291
4	492,655	3,668,104
5	424,155	3,416,251
6	367,361	3,158,776
7	319,194	2,902,138
...
16	53,459	676,076
17	40,488	519,077
18	29,554	384,478
19	19,989	263,990
20	11,073	154,000
...
43	103	2,513
44 ($\delta^*(\mathcal{G})$)	48	1,121

Table 7: k -core decomposition of the Google graph.

k	Number of nodes in k -core	Number of edges in k -core
0	2,745,762	13,965,410
1	2,745,762	13,965,410
2	2,539,676	13,762,533
3	2,299,008	13,295,322
4	2,011,518	12,468,383
5	1,671,474	11,179,712
6	1,284,078	9,363,176
7	888,944	7,164,181
...
14	46,685	717,597
15	35,432	576,755
16	28,153	480,436
17	22,455	400,463
...
63	109	4,232
64 ($\delta^*(\mathcal{G})$)	106	4,043

Table 8: k -core decomposition of the Patent graph.

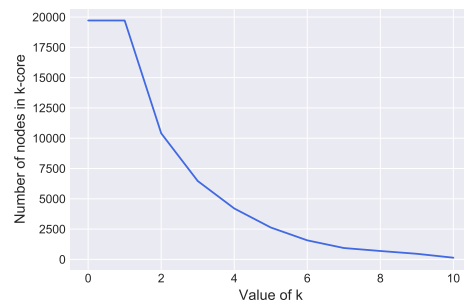


Figure 4: k -core decomposition of the Pubmed graph.

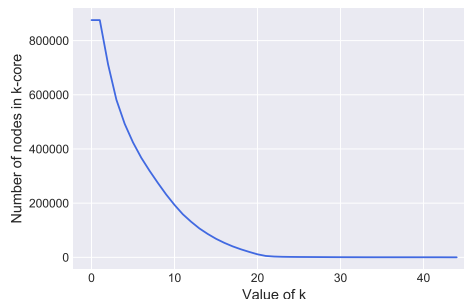


Figure 5: k -core decomposition of the Google graph.

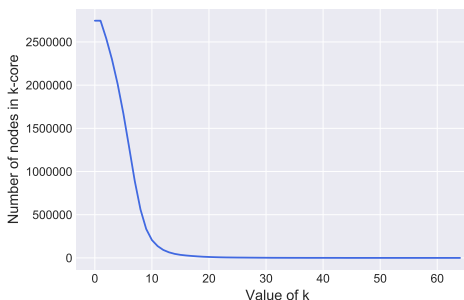


Figure 6: k -core decomposition of the Patent graph.

Annex 2 - Link Prediction

In this Annex 2, we provide complete tables for the *link prediction* task. The main paper discusses the conclusions from experiments; here, we focus on completeness and details regarding our experimental setting.

Medium-size graphs

We applied our framework to all possible subgraphs from the 2-core to the $\delta^*(\mathcal{G})$ -core. We also trained graph AE/VAE models on entire graphs for comparison. Tables 9 to 11 report mean AUC and AP scores and their standard errors over 100 runs (training graphs and masked edges are different for each run) along with mean running times, for the VGAE model. Sizes of k -cores vary over runs due to the edge masking process. We obtained comparable performance/speed trade-offs for graph AE/VAE variants: for brevity, we, therefore, only report results on the 2-core for these models.

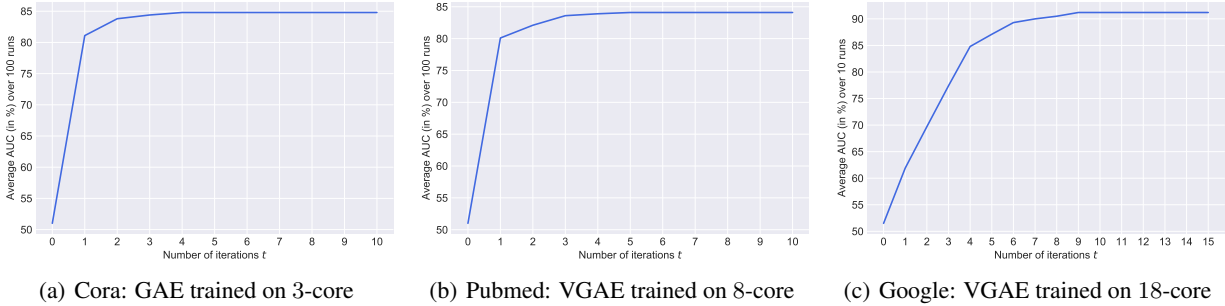


Figure 7: Impact of the number of iterations t during propagation on mean AUC scores.

Large graphs

For the Google and Patent graphs, comparison with models trained on the entire \mathcal{G} was impossible, due to overly large memory requirements. As a consequence, we applied our framework to the five largest k -cores (in terms of nodes) that were tractable using our machines. Tables 12 and 13 report mean AUC/AP scores and standard errors over 10 runs (training graphs and masked edges are different for each run) along with mean running times, for the VGAE model. For other models, we only report results on the second-largest cores for brevity. We chose the second-largest cores (17-core for Google, 15-core for Patent) instead of the largest cores (16-core for Google, 14-core for Patent) to lower running times.

Graph AE/VAE training

All graph AE/VAE models were trained during 200 epochs to return 16-dimensional embeddings, except for Patent (500 epochs, 32-dimensional). We included a 32-dimensional hidden layer in GCN encoders (two for DeepGAE and DeepVGAE), used the Adam optimizer, trained models without dropout, and with a learning rate of 0.01. We performed full-batch gradient descent and used the reparameterization trick [14]. We used the Tensorflow public implementations of these models (see corresponding references). Overall, our setting is quite similar to [16], and we indeed managed to reproduce their scores when training GAE and VGAE on entire graphs, with however larger standard errors. This difference comes from the fact that we used 100 different train/test splits, while they launched all runs on fixed dataset splits (randomness, therefore, only came from the initialization).

Impact of the number of iterations t

We illustrate the impact of the number of iterations t during propagation on performances in Figure 7. We display the evolution of mean AUC scores w.r.t. t , for three different graphs. For $t > 5$ (resp. $t > 10$) in medium-size graphs (resp. large graphs), scores become stable. We specify that the number of iterations has a negligible impact on running times. Therefore, in our experiments, we set $t = 10$ for all models leveraging our degeneracy framework.

Baselines

For DeepWalk [22], we trained models from 10 random walks of length 80 per node with a window size of 5, on a single epoch for each graph. We used similar hyperparameters for

node2vec [11], setting $p = q = 1$, and LINE [27] enforcing second-order proximity. We directly used the public implementations provided by the authors. Due to unstable and underperforming results with 16-dimensional embeddings, we had to increase dimensions up to 64, to compete with autoencoders. For the spectral embedding baseline, we also computed embeddings from 64 Laplacian eigenvectors.

In our experiments, we noticed some slight differences w.r.t. [16] regarding baselines, which we explain by our modifications in train/test splits and by different hyperparameters. However, these slight variations do not impact the conclusions of our experiments. We specify that the spectral embedding baseline is not scalable, due to the required eigen-decomposition of the Laplacian matrix. Moreover, we chose not to report results for DeepWalk on large graphs due to too large training times ($> 20h$) on our machines. This does not question the scalability of this method (which is quite close to node2vec), but it suggests possible improvements in the existing implementation.

Annex 3 - Node Clustering

Lastly, we provide complete tables for the *node clustering* task. As before, we focus on the completeness of results, and refer to the main paper for interpretations.

In experiments, we evaluated the quality of node clustering from latent representations, running k -means in embeddings and reporting normalized *Mutual Information* (MI) scores. We used scikit-learn’s implementation with k -means++ initialization. We do not report any result for the Google graph, due to the lack of ground-truth communities. Also, we obtained very low scores on the Citeseer graph, with all methods, which suggests that node features are more valuable than the graph structure to explain labels. As a consequence, we also omit this graph and focus on Cora, Pubmed, and Patent in Tables 14 to 16. We constructed tables in a similar fashion w.r.t. Annex 2.

Models were trained with identical hyperparameters w.r.t. the *link prediction* task. Contrary to Annex 2, we do not report spectral clustering results because graphs are not connected. Nevertheless, we compared to the “Louvain” method, a popular scalable algorithm to cluster nodes by maximizing the modularity [4], using the Python implementation provided in the python-louvain’s library.

Model	Size of input k -core	Mean Perf. on Test Set (in %)		Mean Running Times (in sec.)			
		AUC	AP	k -core dec.	Model train	Propagation	Total
VGAE on \mathcal{G}	-	84.07 \pm 1.22	87.83 \pm 0.95	-	15.34	-	15.34
on 2-core	1,890 \pm 16	85.24 \pm 1.12	87.37 \pm 1.13	0.16	8.00	0.10	8.26
on 3-core	862 \pm 26	84.53 \pm 1.33	85.04 \pm 1.87	0.16	2.82	0.11	3.09
on 4-core	45 \pm 13	72.33 \pm 4.67	71.98 \pm 4.97	0.16	0.98	0.12	1.26
GAE on 2-core	1,890 \pm 16	85.17 \pm 1.02	87.26 \pm 1.12	0.16	8.05	0.10	8.31
DeepGAE on 2-core	1,890 \pm 16	86.25 \pm 0.81	87.92 \pm 0.78	0.16	8.24	0.10	8.50
DeepVGAE on 2-core	1,890 \pm 16	86.16 \pm 0.95	87.71 \pm 0.98	0.16	8.20	0.10	8.46
Graphite on 2-core	1,890 \pm 16	86.35 \pm 0.82	88.18 \pm 0.84	0.16	9.41	0.10	9.67
Var-Graphite on 2-core	1,890 \pm 16	86.39 \pm 0.84	88.05 \pm 0.80	0.16	9.35	0.10	9.61
ARGA on 2-core	1,890 \pm 16	85.82 \pm 0.88	88.22 \pm 0.70	0.16	7.99	0.10	8.25
ARVGA on 2-core	1,890 \pm 16	85.74 \pm 0.74	88.14 \pm 0.74	0.16	7.98	0.10	8.24
ChebGAE on 2-core	1,890 \pm 16	86.15 \pm 0.54	88.01 \pm 0.39	0.16	15.78	0.10	16.04
ChebVGAE on 2-core	1,890 \pm 16	86.30 \pm 0.49	88.29 \pm 0.50	0.16	15.65	0.10	15.91
GAE with node features on 2-core	1,890 \pm 16	88.10 \pm 0.87	89.36 \pm 0.88	0.16	8.66	0.10	8.92
VGAE with node features on 2-core	1,890 \pm 16	87.97 \pm 0.99	89.53 \pm 0.96	0.16	8.60	0.10	8.86
DeepWalk	-	83.02 \pm 1.21	84.41 \pm 1.23	-	38.50	-	38.50
LINE	-	83.49 \pm 1.31	84.42 \pm 1.39	-	11.55	-	11.55
node2vec	-	83.52 \pm 1.47	84.60 \pm 1.23	-	8.42	-	8.42
Spectral	-	86.53 \pm 1.02	87.41 \pm 1.12	-	2.78	-	2.78

Table 9: Link prediction on Cora ($n = 2,708$, $m = 5,429$), using VGAE on all cores, graph AE/VAE variants on 2-core, and baselines.

Model	Size of input k -core	Mean Perf. on Test Set (in %)		Mean Running Times (in sec.)			
		AUC	AP	k -core dec.	Model train	Propagation	Total
VGAE on \mathcal{G}	-	78.10 \pm 1.52	83.12 \pm 1.03	-	22.40	-	22.40
on 2-core	1,306 \pm 19	77.50 \pm 1.59	81.92 \pm 1.41	0.15	4.72	0.11	4.98
on 3-core	340 \pm 13	76.40 \pm 1.72	80.22 \pm 1.42	0.15	1.75	0.14	2.04
on 4-core	139 \pm 13	73.34 \pm 2.43	75.49 \pm 2.39	0.15	1.16	0.16	1.47
on 5-core	46 \pm 10	65.47 \pm 3.16	68.50 \pm 2.77	0.15	0.99	0.16	1.30
GAE on 2-core	1,306 \pm 19	78.35 \pm 1.51	82.44 \pm 1.32	0.15	4.78	0.11	5.04
DeepGAE on 2-core	1,306 \pm 19	79.32 \pm 1.39	82.80 \pm 1.33	0.15	4.99	0.11	5.25
DeepVGAE on 2-core	1,306 \pm 19	78.52 \pm 1.02	82.43 \pm 0.97	0.15	4.95	0.11	5.21
Graphite on 2-core	1,306 \pm 19	78.61 \pm 1.58	82.81 \pm 1.24	0.15	5.88	0.11	6.14
Var-Graphite on 2-core	1,306 \pm 19	78.51 \pm 1.62	82.72 \pm 1.25	0.15	5.86	0.11	6.12
ARGA on 2-core	1,306 \pm 19	78.89 \pm 1.33	82.89 \pm 1.03	0.15	4.54	0.11	4.80
ARVGA on 2-core	1,306 \pm 19	77.98 \pm 1.39	82.39 \pm 1.09	0.15	4.40	0.11	4.66
ChebGAE on 2-core	1,306 \pm 19	78.62 \pm 0.95	83.22 \pm 0.89	0.15	8.87	0.11	9.13
ChebVGAE on 2-core	1,306 \pm 19	78.75 \pm 1.03	83.23 \pm 0.76	0.15	8.75	0.11	9.01
GAE with node features on 2-core	1,306 \pm 19	81.21 \pm 1.86	83.99 \pm 1.52	0.15	5.51	0.11	5.77
VGAE with node features on 2-core	1,306 \pm 19	81.88 \pm 2.23	83.83 \pm 1.85	0.15	5.70	0.11	5.96
DeepWalk	-	76.92 \pm 1.15	79.30 \pm 0.79	-	41.20	-	41.20
LINE	-	77.12 \pm 1.09	79.92 \pm 0.80	-	12.41	-	12.41
node2vec	-	76.98 \pm 1.27	79.74 \pm 0.84	-	9.98	-	9.98
Spectral	-	80.56 \pm 1.41	83.98 \pm 1.08	-	3.77	-	3.77

Table 10: Link prediction on Citeseer ($n = 3,327$, $m = 4,732$), using VGAE on all cores*, graph AE/VAE variants on 2-core, and baselines.
* 6-core and 7-core are not reported due to their frequent vanishing after edge masking.

Model	Size of input k -core	Mean Perf. on Test Set (in %)		Mean Running Times (in sec.)			
		AUC	AP	k -core dec.	Model train	Propagation	Total
VGAE on \mathcal{G}	-	83.02 \pm 0.13	87.55 \pm 0.18	-	710.54	-	710.54
on 2-core	9,277 \pm 25	83.97 \pm 0.39	85.80 \pm 0.49	1.35	159.15	0.31	160.81
on 3-core	5,551 \pm 19	83.92 \pm 0.44	85.49 \pm 0.71	1.35	60.12	0.34	61.81
on 4-core	3,269 \pm 30	82.40 \pm 0.66	83.39 \pm 0.75	1.35	22.14	0.36	23.85
on 5-core	1,843 \pm 25	78.31 \pm 1.48	79.21 \pm 1.64	1.35	7.71	0.36	9.42
...
on 8-core	414 \pm 89	67.27 \pm 1.65	67.65 \pm 2.00	1.35	1.55	0.38	3.28
on 9-core	149 \pm 93	61.92 \pm 2.88	63.97 \pm 2.86	1.35	1.14	0.38	2.87
GAE on 2-core	9,277 \pm 25	84.30 \pm 0.27	86.11 \pm 0.43	1.35	167.25	0.31	168.91
DeepGAE on 2-core	9,277 \pm 25	84.61 \pm 0.54	85.18 \pm 0.57	1.35	166.38	0.31	168.04
DeepVGAE on 2-core	9,277 \pm 25	84.46 \pm 0.46	85.31 \pm 0.45	1.35	157.43	0.31	159.09
Graphite on 2-core	9,277 \pm 25	84.51 \pm 0.58	85.65 \pm 0.58	1.35	167.88	0.31	169.54
Var-Graphite on 2-core	9,277 \pm 25	84.30 \pm 0.57	85.57 \pm 0.58	1.35	158.16	0.31	159.82
ARGA on 2-core	9,277 \pm 25	84.37 \pm 0.54	86.07 \pm 0.45	1.35	164.06	0.31	165.72
ARVGA on 2-core	9,277 \pm 25	84.10 \pm 0.53	85.88 \pm 0.41	1.35	155.83	0.31	157.49
ChebGAE on 2-core	9,277 \pm 25	84.63 \pm 0.42	86.05 \pm 0.70	1.35	330.37	0.31	332.03
ChebVGAE on 2-core	9,277 \pm 25	84.54 \pm 0.48	86.00 \pm 0.63	1.35	320.01	0.31	321.67
GAE with node features on 2-core	9,277 \pm 25	84.94 \pm 0.54	85.83 \pm 0.58	1.35	168.62	0.31	170.28
VGAE with node features on 2-core	9,277 \pm 25	85.81 \pm 0.68	88.01 \pm 0.53	1.35	164.10	0.31	165.76
DeepWalk	-	81.04 \pm 0.45	84.04 \pm 0.51	-	342.25	-	342.25
LINE	-	81.21 \pm 0.31	84.60 \pm 0.37	-	63.52	-	63.52
node2vec	-	81.25 \pm 0.26	85.55 \pm 0.26	-	48.91	-	48.91
Spectral	-	83.14 \pm 0.42	86.55 \pm 0.41	-	31.71	-	31.71

Table 11: Link prediction on Pubmed ($n = 19,717$, $m = 44,338$), using VGAE on all cores*, graph AE/VAE variants on 2-core, and baselines. * 10-core is not reported due to its frequent vanishing after edge masking.

Model	Size of input k -core	Mean Perf. on Test Set (in %)		Mean Running Times (in sec.)			
		AUC	AP	k -core dec.	Model train	Propagation	Total
VGAE on 16-core	36,854 \pm 132	93.56 \pm 0.38	93.34 \pm 0.31	301.16	2,695.42	25.54	3,022.12 (50min)
on 17-core	23,787 \pm 208	93.22 \pm 0.40	93.20 \pm 0.45	301.16	1,001.64	28.16	1,330.86 (22min)
on 18-core	13,579 \pm 75	91.24 \pm 0.40	92.34 \pm 0.51	301.16	326.76	28.20	656.12 (11min)
on 19-core	6,613 \pm 127	87.79 \pm 0.31	89.13 \pm 0.29	301.16	82.19	28.59	411.94 (7min)
on 20-core	3,589 \pm 106	81.74 \pm 1.17	83.51 \pm 1.22	301.16	25.59	28.50	355.55 (6 min)
GAE on 17-core	23,787 \pm 208	94.02 \pm 0.20	94.31 \pm 0.21	301.16	1,073.18	28.16	1,402.50 (23min)
DeepGAE on 17-core	23,787 \pm 208	93.74 \pm 0.17	92.94 \pm 0.33	301.16	1,137.24	28.16	1,466.56 (24min)
DeepVGAE on 17-core	23,787 \pm 208	93.12 \pm 0.29	92.71 \pm 0.29	301.16	1,088.41	28.16	1,417.73 (24min)
Graphite on 17-core	23,787 \pm 208	93.29 \pm 0.33	93.11 \pm 0.42	301.16	1,033.21	28.16	1,362.53 (23min)
Var-Graphite on 17-core	23,787 \pm 208	93.13 \pm 0.35	92.90 \pm 0.39	301.16	989.90	28.16	1,319.22 (22min)
ARGA on 17-core	23,787 \pm 208	93.82 \pm 0.17	94.17 \pm 0.18	301.16	1,053.95	28.16	1,383.27 (23min)
ARVGA on 17-core	23,787 \pm 208	93.00 \pm 0.17	93.38 \pm 0.19	301.16	1,027.52	28.16	1,356.84 (23min)
ChebGAE on 17-core	23,787 \pm 208	95.24 \pm 0.26	96.94 \pm 0.27	301.16	2,120.66	28.16	2,449.98 (41min)
ChebVGAE on 17-core	23,787 \pm 208	95.03 \pm 0.25	96.82 \pm 0.72	301.16	2,086.07	28.16	2,415.39 (40min)
LINE	-	93.52 \pm 0.43	95.90 \pm 0.59	-	19,699.02	-	19,699.02 (5h19)
node2vec	-	94.89 \pm 0.63	96.82 \pm 0.72	-	14,762.78	-	14,762.78 (4h06)

Table 12: Link prediction on Google ($n = 875,713$, $m = 4,322,051$), using VGAE on 16 to 20 cores, graph AE/VAE variants on 17-core, and baselines.

Model	Size of input k -core	Mean Perf. on Test Set (in %)		Mean Running Times (in sec.)			
		AUC	AP	k -core dec.	Model train	Propagation	Total
VGAE on 14-core	38,408 \pm 147	88.48 \pm 0.35	88.81 \pm 0.32	507.08	3,024.31	122.29	3,653.68 (1h01)
on 15-core	29,191 \pm 243	88.16 \pm 0.50	88.37 \pm 0.57	507.08	1,656.46	123.47	2,287.01 (38min)
on 16-core	23,132 \pm 48	87.85 \pm 0.47	88.02 \pm 0.48	507.08	948.09	124.26	1,579.43 (26min)
on 17-core	18,066 \pm 143	87.34 \pm 0.56	87.64 \pm 0.47	507.08	574.25	126.55	1,207.88 (20min)
on 18-core	13,972 \pm 86	87.27 \pm 0.55	87.78 \pm 0.51	507.08	351.73	127.01	985.82 (16min)
GAE on 15-core	29,191 \pm 243	87.59 \pm 0.29	87.30 \pm 0.28	507.08	1,880.11	123.47	2,510.66 (42min)
DeepGAE on 15-core	29,191 \pm 243	87.71 \pm 0.31	87.64 \pm 0.19	507.08	2,032.15	123.47	2,662.70 (44min)
DeepVGAE on 15-core	29,191 \pm 243	87.03 \pm 0.54	87.20 \pm 0.44	507.08	1,927.33	123.47	2,557.88 (43min)
Graphite on 15-core	29,191 \pm 243	85.19 \pm 0.38	86.01 \pm 0.31	507.08	1,989.72	123.47	2,620.27 (44min)
Var-Graphite on 15-core	29,191 \pm 243	85.37 \pm 0.30	86.07 \pm 0.24	507.08	1,916.79	123.47	2,547.34 (42min)
ARGA on 15-core	29,191 \pm 243	89.22 \pm 0.10	89.40 \pm 0.11	507.08	2,028.46	123.47	2,659.01 (44min)
ARVGA on 15-core	29,191 \pm 243	87.18 \pm 0.17	87.39 \pm 0.33	507.08	1,915.53	123.47	2,546.08 (42min)
ChebGAE on 15-core	29,191 \pm 243	88.53 \pm 0.20	88.91 \pm 0.20	507.08	3,391.01	123.47	4,021.56 (1h07)
ChebVGAE on 15-core	29,191 \pm 243	88.75 \pm 0.19	89.07 \pm 0.24	507.08	3,230.52	123.47	3,861.07 (1h04)
LINE	-	90.07 \pm 0.41	94.52 \pm 0.49	-	33,063.80	-	33,063.80 (9h11)
node2vec	-	95.04 \pm 0.25	96.01 \pm 0.19	-	26,126.01	-	26,126.01 (7h15)

Table 13: Link prediction on Patent ($n = 2,745,762$, $m = 13,965,410$), using VGAE on 14 to 18 cores, graph AE/VAE variants on 15-core, and baselines.

Model	Size of input k -core	Mean Performance (in %)	Mean Running Times (in sec.)			
			k -core dec.	Model train	Propagation	Total
VGAE on \mathcal{G}	-	29.52 \pm 2.61	-	15.34	-	15.34
on 2-core	2,136	34.08 \pm 2.55	0.16	9.94	0.10	10.20
on 3-core	1,257	36.29 \pm 2.52	0.16	4.43	0.11	4.70
on 4-core	174	35.93 \pm 1.88	0.16	1.16	0.12	1.44
VGAE with node features on \mathcal{G}	-	47.25 \pm 1.80	-	15.89	-	15.89
on 2-core	2,136	45.09 \pm 1.91	0.16	10.42	0.10	10.68
on 3-core	1,257	40.96 \pm 2.06	0.16	4.75	0.11	5.02
on 4-core	174	38.11 \pm 1.23	0.16	1.22	0.12	1.50
GAE on 2-core	2,136	34.91 \pm 2.51	0.16	10.02	0.10	10.28
DeepGAE on 2-core	2,136	35.30 \pm 2.52	0.16	10.12	0.10	10.38
DeepVGAE on 2-core	2,136	34.49 \pm 2.85	0.16	10.09	0.10	10.35
Graphite on 2-core	2,136	33.91 \pm 2.17	0.16	10.97	0.10	11.23
Var-Graphite on 2-core	2,136	33.89 \pm 2.13	0.16	10.91	0.10	11.17
ARGA on 2-core	2,136	34.73 \pm 2.84	0.16	9.99	0.10	10.25
ARVGA on 2-core	2,136	33.36 \pm 2.53	0.16	9.97	0.10	10.23
ChebGAE on 2-core	2,136	36.52 \pm 2.05	0.16	19.22	0.10	19.48
ChebVGAE on 2-core	2,136	37.83 \pm 2.11	0.16	20.13	0.10	20.39
DeepWalk	-	40.37 \pm 1.51	-	38.50	-	38.50
LINE	-	39.78 \pm 1.24	-	11.55	-	11.55
Louvain	-	46.76 \pm 0.82	-	1.83	-	1.83
node2vec	-	43.45 \pm 1.32	-	8.42	-	8.42

Table 14: Node clustering on Cora ($n = 2,708$, $m = 5,429$), using VGAE on all cores, graph AE/VAE variants on 2-core, and baselines.

Model	Size of input <i>k</i> -core	Mean Performance (in %)	Mean Running Times (in sec.)			
		MI	<i>k</i> -core dec.	Model train	Propagation	Total
VGAE on \mathcal{G}	-	22.36 ± 0.25	-	707.77	-	707.77
on 2-core	10,404	23.71 ± 1.83	1.35	199.07	0.30	200.72
on 3-core	6,468	25.19 ± 1.59	1.35	79.26	0.34	80.95
on 4-core	4,201	24.67 ± 3.87	1.35	34.66	0.35	36.36
on 5-core	2,630	17.90 ± 3.76	1.35	14.55	0.36	16.26
...
on 10-core	137	10.79 ± 1.16	1.35	1.15	0.38	2.88
VGAE with node features on \mathcal{G}	-	26.05 ± 1.40	-	708.59	-	708.59
on 2-core	10,404	24.25 ± 1.92	1.35	202.37	0.30	204.02
on 3-core	6,468	23.26 ± 3.42	1.35	82.89	0.34	84.58
on 4-core	4,201	20.17 ± 1.73	1.35	36.89	0.35	38.59
on 5-core	2,630	18.15 ± 2.04	1.35	16.08	0.36	17.79
...
on 10-core	137	11.67 ± 0.71	1.35	0.97	0.38	2.70
GAE on 2-core	10,404	22.76 ± 2.25	1.35	203.56	0.30	205.21
DeepGAE on 2-core	10,404	24.53 ± 3.30	1.35	205.11	0.30	206.76
DeepVGAE on 2-core	10,404	25.63 ± 3.51	1.35	200.73	0.30	202.38
Graphite on 2-core	10,404	26.55 ± 2.17	1.35	209.12	0.30	210.77
Var-Graphite on 2-core	10,404	26.69 ± 2.21	1.35	200.86	0.30	202.51
ARGA on 2-core	10,404	23.68 ± 3.18	1.35	207.50	0.30	209.15
ARVGA on 2-core	10,404	25.98 ± 1.93	1.35	199.94	0.30	201.59
ChebGAE on 2-core	10,404	25.88 ± 1.66	1.35	410.81	0.30	412.46
ChebVGAE on 2-core	10,404	26.50 ± 1.49	1.35	399.96	0.30	401.61
DeepWalk	-	27.23 ± 0.32	-	342.25	-	342.25
LINE	-	26.26 ± 0.28	-	63.52	-	63.52
Louvain	-	23.02 ± 0.47	-	27.32	-	27.32
node2vec	-	29.57 ± 0.22	-	48.91	-	48.91

Table 15: Node clustering on Pubmed ($n = 19,717$, $m = 44,338$), using VGAE on all cores, Graph AE/VAE variants on 2-core, and baselines.

Model	Size of input <i>k</i> -core	Mean Performance (in %)	Mean Running Times (in sec.)			
		MI	<i>k</i> -core dec.	Model train	Propagation	Total
VGAE on 14-core	46,685	25.22 ± 1.51	507.08	6,390.37	120.80	7,018.25 (1h57)
on 15-core	35,432	24.53 ± 1.62	507.08	2,589.95	123.95	3,220.98 (54min)
on 16-core	28,153	24.16 ± 1.96	507.08	1,569.78	123.14	2,200.00 (37min)
on 17-core	22,455	24.14 ± 2.01	507.08	898.27	124.02	1,529.37 (25min)
on 18-core	17,799	22.54 ± 1.98	507.08	551.83	126.67	1,185.58 (20min)
GAE on 15-core	35,432	23.76 ± 2.25	507.08	2,750.09	123.95	3,381.13 (56min)
DeepGAE on 15-core	35,432	24.27 ± 1.10	507.08	3,007.31	123.95	3,638.34 (1h01)
DeepVGAE on 15-core	35,432	24.54 ± 1.23	507.08	2,844.16	123.95	3,475.19 (58min)
Graphite on 15-core	35,432	24.22 ± 1.45	507.08	2,899.87	123.95	3,530.90 (59min)
Var-Graphite on 15-core	35,432	24.25 ± 1.51	507.08	2,869.92	123.95	3,500.95 (58min)
ARGA on 15-core	35,432	24.26 ± 1.18	507.08	3,013.28	123.95	3,644.31 (1h01)
ARVGA on 15-core	35,432	24.76 ± 1.32	507.08	2,862.54	123.95	3,493.57 (58min)
ChebGAE on 15-core	35,432	25.23 ± 1.21	507.08	5,412.12	123.95	6,043.15 (1h41)
ChebVGAE on 15-core	35,432	25.30 ± 1.22	507.08	5,289.91	123.95	5,920.94 (1h38)
LINE	-	23.19 ± 1.82	-	33,063.80	-	33,063.80 (9h11)
Louvain	-	11.99 ± 1.79	-	13,634.16	-	13,634.16 (3h47)
node2vec	-	24.10 ± 1.64	-	26,126.01	-	26,126.01 (7h15)

Table 16: Node clustering on Patent ($n = 2,745,762$, $m = 13,965,410$), using VGAE on 14 to 18 cores, graph AE/VAE variants on 15-core, and baselines.